Research Article | Vol. 25, No. 26 | 25 Dec 2017 | OPTICS EXPRESS 33193
Optics EXPRESS

Highly-sensitive optical biosensor based on equal FSR cascaded microring resonator with intensity interrogation for detection of progesterone molecules

ZHENYI XIE,[1] ZIWEI CAO,[1] YONG LIU,[1] QINGWEN ZHANG,[2,3] JUN ZOU,[4] LIYANG SHAO,[5,6] YI WANG,[2,3,7] JIANJUN HE,[1] AND MINGYU LI[1,*]

[1]*State Key Laboratory of Modern Optical Instrumentation, Centre for Integrated Optoelectronics, College of Optical Science and Engineering, Zhejiang University, Hangzhou 310027, China*
[2]*Wenzhou Institute of Biomaterials and Engineering, Chinese Academy of Sciences, Wenzhou 325001, China*
[3]*School of Biomedical Engineering, Wenzhou Medical University, Wenzhou 325001, China*
[4]*College of Science, Zhejiang University of Technology, Hangzhou 310023, China*
[5]*Department of Electrical and Electronic Engineering, Southern University of Science and Technology, Shenzhen 518055, China*
[6]*shaoly@sustc.edu.cn*
[7]*wangyi@wibe.ac.cn*
**limy@zju.edu.cn*

Abstract: We report a refractive index sensing system with a high sensitivity of 1579 dB/RIU and a low refractive index detection limit of 9.7×10^{-6} RIU. The sensing system was based on cascaded-microring resonators (CMRR) using intensity interrogation. The free spectrum range (FSR) for the reference ring was designed to be equal to the sensing ring. The sensing ring of the CMRR was modified with molecularly imprinted polymers (MIPs) for the detection of progesterone. The achieved limit of detection (LOD) was as low as 83.5 fg/mL.

OCIS codes: (130.0130) Integrated optics; (170.0170) Medical optics and biotechnology; (280.0280) Remote sensing and sensors.

References and links

1. B. Sepúlveda, J. S. Río, M. Moreno, F. J. Blanco, K. Mayora, C. Domínguez, and L. M. Lechuga, "Optical biosensor microsystems based on the integration of highly sensitive Mach Zehnder interferometer devices," J. Opt. A, Pure Appl. Opt. **8**(7), S561–S566 (2006).
2. X. Han, Y. Shao, X. Han, Z. Lu, Z. Wu, J. Teng, J. Ren, and M. Zhao, "Athermal optical waveguide microring biosensor with intensity interrogation," Opt. Commun. **356**, 41–48 (2015).
3. M. R. Lee and P. M. Fauchet, "Nanoscale microcavity sensor for single particle detection," Opt. Lett. **32**(22), 3284–3286 (2007).
4. C. A. Barrios, "Integrated microring resonator sensor arrays for labs-on-chips," Anal. Bioanal. Chem. **403**(6), 1467–1475 (2012).
5. L. Qin, L. Wang, M. Li, and J.-J. He, "Optical Sensor Based on Vernier-Cascade of Ring Resonator and Echelle Diffraction Grating," IEEE Photonics Technol. Lett. **24**(11), 954–956 (2012).
6. A. Densomore, D. X. Xu, P. Waldron, S. Janz, A. Delâge, and P. Cheben, "Silicon Microphotonic Waveguides for Biological Sensing," in *Proceedings of IEEE Conference on Biophotonics, Nanophotonics and Metamaterials* (IEEE, 2006), pp. 15–18.
7. J. Homola, "Surface plasmon resonance sensors for detection of chemical and biological species," Chem. Rev. **108**(2), 462–493 (2008).
8. R. W. Boyd and J. E. Heebner, "Sensitive disk resonator photonic biosensor," Appl. Opt. **40**(31), 5742–5747 (2001).
9. X. Fan, I. M. White, S. I. Shopova, H. Zhu, J. D. Suter, and Y. Sun, "Sensitive optical biosensors for unlabeled targets: A review," Anal. Chim. Acta **620**(1-2), 8–26 (2008).
10. X. Sun, D. Dai, L. Thylén, and L. Wosinski, "High-sensitivity liquid refractive-index sensor based on a Mach-Zehnder interferometer with a double-slot hybrid plasmonic waveguide," Opt. Express **23**(20), 25688–25699 (2015).

#312903 https://doi.org/10.1364/OE.25.033193
Journal © 2017 Received 7 Nov 2017; revised 7 Dec 2017; accepted 8 Dec 2017; published 20 Dec 2017

Optics EXPRESS

11. T. Lu, H. Lee, T. Chen, S. Herchak, J. H. Kim, S. E. Fraser, R. C. Flagan, and K. Vahala, "High sensitivity nanoparticle detection using optical microcavities," Proc. Natl. Acad. Sci. U.S.A. **108**(15), 5976–5979 (2011).
12. M. D. Baaske, M. R. Foreman, and F. Vollmer, "Single-molecule nucleic acid interactions monitored on a label-free microcavity biosensor platform," Nat. Nanotechnol. **9**(11), 933–939 (2014).
13. W. Yu, W. C. Jiang, Q. Lin, and T. Lu, "Cavity optomechanical spring sensing of single molecules," Nat. Commun. **7**, 12311 (2016).
14. L. Jin, M. Li, and J.-J. He, "Highly sensitive optical sensor based on two cascaded micro-ring resonators with an LED light source," Proc. SPIE **7943**, 794307 (2011).
15. X. Jiang, J. Ye, J. Zou, M. Li, and J.-J. He, "Cascaded silicon-on-insulator double-ring sensors operating in high-sensitivity transverse-magnetic mode," Opt. Lett. **38**(8), 1349–1351 (2013).
16. Y. Chen, F. Yu, C. Yang, J. Song, L. Tang, M. Li, and J.-J. He, "Label-free biosensing using cascaded double-microring resonators integrated with microfluidic channels," Opt. Commun. **344**, 129–133 (2015).
17. E. B. Fonseca, E. Celik, M. Parra, M. Singh, and K. H. Nicolaides, "Progesterone and the risk of preterm birth among women with a short cervix," N. Engl. J. Med. **357**(5), 462–469 (2007).
18. J. Brolin, L. Skoog, and P. Ekman, "Immunohistochemistry and biochemistry in detection of androgen, progesterone, and estrogen receptors in benign and malignant human prostatic tissue," Prostate **20**(4), 281–295 (1992).
19. L. Meijer, A. Borgne, O. Mulner, J. P. J. Chong, J. J. Blow, N. Inagaki, M. Inagaki, J.-G. Delcros, and J.-P. Moulinoux, "Biochemical and Cellular Effects of Roscovitine, a Potent and Selective Inhibitor of the Cyclin-Dependent Kinases cdc2, cdk2 and cdk5," Eur. J. Biochem. **243**(1-2), 527–536 (1997).
20. Q. Zhang, L. Jing, J. Zhang, Y. Ren, Y. Wang, Y. Wang, T. Wei, and B. Liedberg, "Surface plasmon resonance sensor for femtomolar detection of testosterone with water-compatible macroporous molecularly imprinted film," Anal. Biochem. **463**(1), 7–14 (2014).
21. L. Chen, S. Xu, and J. Li, "Recent advances in molecular imprinting technology: current status, challenges and highlighted applications," Chem. Soc. Rev. **40**(5), 2922–2942 (2011).
22. A. Bossi, F. Bonini, A. P. Turner, and S. A. Piletsky, "Molecularly imprinted polymers for the recognition of proteins: the state of the art," Biosens. Bioelectron. **22**(6), 1131–1137 (2007).
23. L. Jin, M. Li, and J.-J. He, "Analysis of wavelength and intensity interrogation methods in cascaded double-ring sensors," J. Lightwave Technol. **30**(12), 1994–2002 (2012).
24. L. Wu, C. Xu, C. Xia, Y. Duan, C. Xu, H. Zhang, and J. Bao, "Development and Application of an ELISA Kit for the Detection of Milk Progesterone in Dairy Cows," Monoclon. Antib. Immunodiagn. Immunother. **33**(5), 330–333 (2014).
25. J. V. Samsonova, V. A. Safronova, and A. P. Osipov, "Pretreatment-free lateral flow enzyme immunoassay for progesterone detection in whole cows' milk," Talanta **132**, 685–689 (2015).

1. Introduction

Mach-Zehnder interferometers (MZI) [1,2], photonic crystal (PhC) [3], microring resonator [4–6], surface plasmon resonance [7] and micro-disks [8] are widely used in optical waveguide-based biosensors [9]. Intensity interrogation and wavelength interrogation are two typical sensing methods for the optical waveguide sensors. To achieve the high sensitivity and the low noise level for traditional MZIs [10], the highly sensitive power sensors and the ultra-stable systems (especially for temperature controlling) are required in the intensity interrogation, while the stable light sources and the high resolution spectrometers are required in the wavelength interrogation. The bandgap of waveguides based PhC sensors is formed by the periodic dielectric structure. In 2007, Lee and Fauchet [3] demonstrated that the PhC sensor is capable of detecting ~1 fg of matter. However, the small feature size pattern of the device requires a high precision lithography process, which prevented these research results from being commercialized. For high-sensitivity micro-cavity resonators, sharp resonance peaks can be achieved by designing the Q factor to be larger than 10^8 [11]. Recent years have witnessed significant progress in making whispering gallery microcavities (WGM) sensors with high sensitivity due to the ultra-high Q cavities [11–13]. However, these sensing systems required the tunable laser sources with a narrow bandwidth and a high stability, which can be hardly integrated onto one chip. Using Vernier effects in the CMRR turned out to be an effective alternative to alleviate the above problems. Recently, we demonstrated silicon-on-insulator (SOI) sensors based on CMRR with high-sensitivity of 24300 nm/RIU for wavelength interrogation and 2430 dB/RIU for intensity interrogation [14,15]. Though the sensitivity is not as good as that of the ultra-high Q cavity sensors [11–13] yet, no complex instruments are required and the CMRR has been successfully integrated with microfluidic channels for kinetic measurements of molecular interaction [16].

Optics EXPRESS

In this paper, we further apply the system for the detection of progesterone as a model experiment based on MIPs. Progesterone plays an important role in human health, especially for women with a short cervix. Treatment with progesterone can reduce the rate of spontaneous early preterm delivery [17]. Immunoassays [18] and chromatography [19] are two primary methods for progesterone analysis. The sensitivity of immunoassays heavily relies on the antibody activity that have limited thermal stability, whereas the chromatography suffers from the weak specificity and insufficient sensitivity [20]. Molecularly imprinted are widely applied in sensor modification in recent years [21]. Specific recognition sites were obtained by removing template molecules from the polymers [22] constructed by light polymerization or heat polymerization. Here, a CMRR was designed with nearly the same free spectrum ranges of the reference ring (FSRr) and sensing ring (FSRs). A complete system was constructed with intensity interrogation for the measurement of intensity variations based on the refractive index changes. Modified with MIPs [20] for the detection of progesterone, the achieved LOD was as low as 83.5 fg/mL.

2. Experiments

2.1 Materials

Acetic acid, Methacrylic acid (MAA), Ethylene glycol dimethacrylate (EGDMA) and Benzophenone were purchased from Sigma-Aldrich. Testosterone, progesterone and all the other reagents were purchased from Sinopharm Chemical Reagent Co. Ltd (Shanghai, China).

2.2 Fabrication of CMRR chip

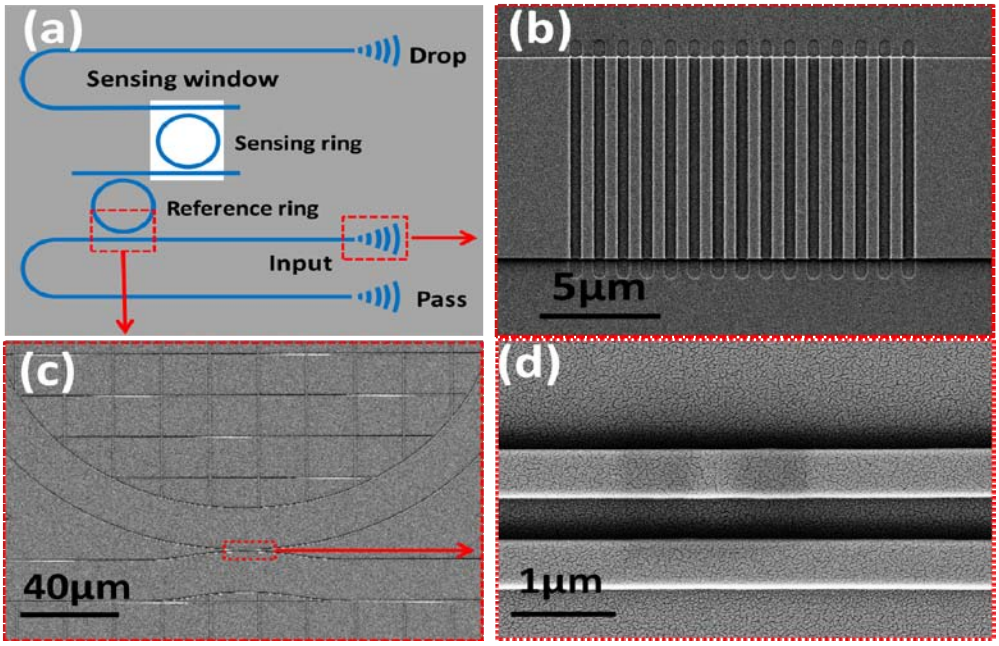

Fig. 1. (a) Schematic image of the CMRR sensor; (b) SEM image of the grating coupler; (c) SEM image of sensing ring; (d) SEM image of the directional coupler.

A standard SOI wafer with a 220 nm-thick silicon top layer and a 2 μm-thick buried oxide was used. Waveguides and ring patterns were defined by standard stepper lithography and inductive coupled plasma etching. A schematic image of the CMRR sensor is shown in Fig. 1(a). After the patterning, the whole chip was passivated by 1.8 μm-thick SU8 as the upper cladding, and the sensing ring was exposed to the reagent sample by removing the upper cladding layer in the sensing widow. SEM images of the fabricated grating coupler, sensing

ring and the gap of the directional coupler are shown in Figs. 1(b)-1(d), respectively. The radii of the reference ring and sensing ring were measured to be 128 μm and 125.5 μm, respectively. These facilitate to achieve similar values of FSRr and FSRs. Figure 1(b) is the SEM image of TM grating coupler with an etch depth of 150 nm, a period of 1 μm and a duty cycle of 50%. The gap of the directional coupler is 500 nm.

2.3 Sensing ring functionalized with MIPs

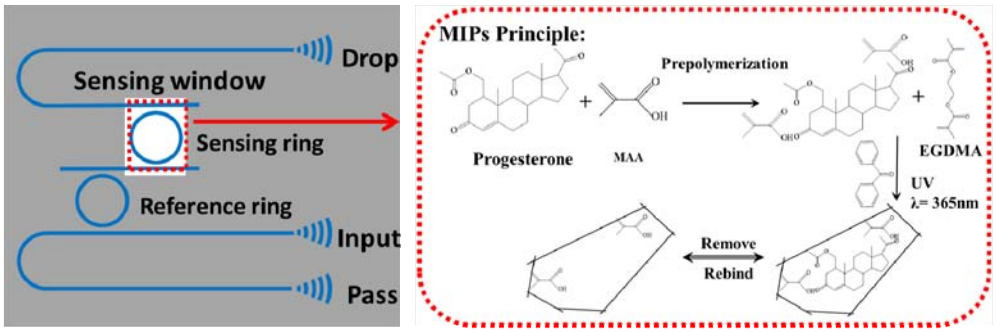

Fig. 2. Progesterone-MIPs synthesized on the chip and the MIPs principle

The progesterone-MIPs was then synthesized based on UV photo polymerization [20]. A schematic illustration of the principle of MIPs and procedures of synthesis were presented in Fig. 2. In the experiment, the CMRR chip was cleaned in ethanol by ultrasonic for 15 min, rinsed by deionized (DI) water and then dried using nitrogen. The reaction solution consists of 8.4 mg of progesterone, 8.8 μL of MAA and 2.52 mL of ethanol. The sample was sonicated for 5 min and then pre-polymerized for 3 h at room temperature. Then, 57 μL of cross-linker EGDMA and 8 mg of benzophenone as initiator were added to the reaction solution. Subsequently, nitrogen is slowly injected into the reaction solution to remove oxygen for 10 min. Then, the solution was dripped in the homemade solution tank (2 mm × 18 mm × 1 mm) and the tank was covered with a glass which is nearly transparent for UV irradiation (λ = 365 nm). Finally, the chip with the solution tank will be placed under UV irradiation for 30 min.

Meanwhile, a non-imprinted polymer films (NIPs) CMRR chip without using the progesterone as template molecule was simultaneously prepared. Through the control experiment, the specificity of the MIPs-CMRR sensor chip can be analyzed.

2.4 Sensor system assembly

The sensor system was then assembled by packaging the chip with fiber array (FA). As shown in Fig. 3(a), the FA was fixed on the six-dimensional positioning stage and the chip was fixed on the three-dimensional nanopositioning stage. To measure the spectrum of the sensor system, the TM polarized light from the tunable light source (Agilent 81600B) was coupled into input waveguide of the chip by a polarization controller and the output light was collected by the power meter (Agilent 81635A).

Optics EXPRESS

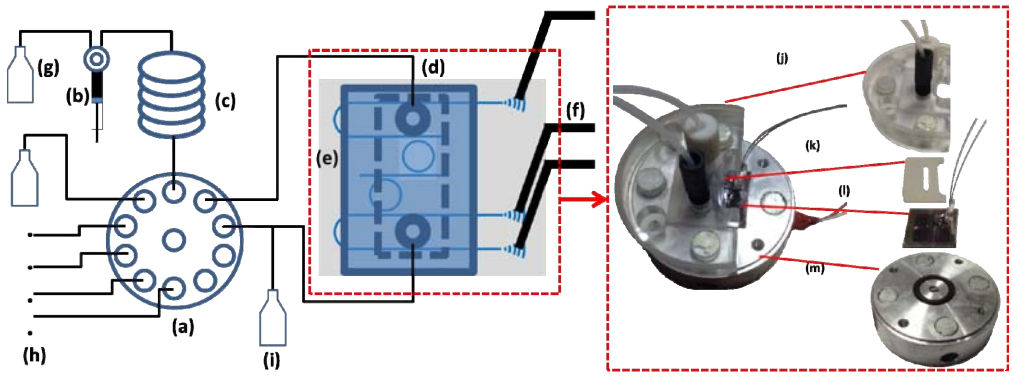

Fig. 3. (a, b) Multi-channels valve and injection pump will be controlled by computer; (c) long ring pipe for liquid storage; (d) microfluidic channel constructed by PMMA and TEC; (e) chip; (f) fiber array; (g, h, i) glass bottle for DI water, sample, waste liquid storage; (j) PMMA lid (k) rubber channel; (l) the packaged chip; (m) metal block integrated with a temperature controller.

Figures 3(a)-3(i) show the schematic of the pump system. The system is composed of a multi-channels valve, an injection pump, a long ring pipe for liquid storage, a microfluidic channel, and a CMRR chip based on SOI optical waveguide. A broadband source, two power detectors (PD), a signal acquisition circuit (SAC), and a controlling computer were used to perform the intensity interrogation. Figures 3(j)-3(m) show the picture of the microfluidic channel. The channel comprises of a PMMA lid, a silica gel channel, a packaged chip, and a metal block integrated with a temperature controller.

Optics EXPRESS

3. Results and discussion

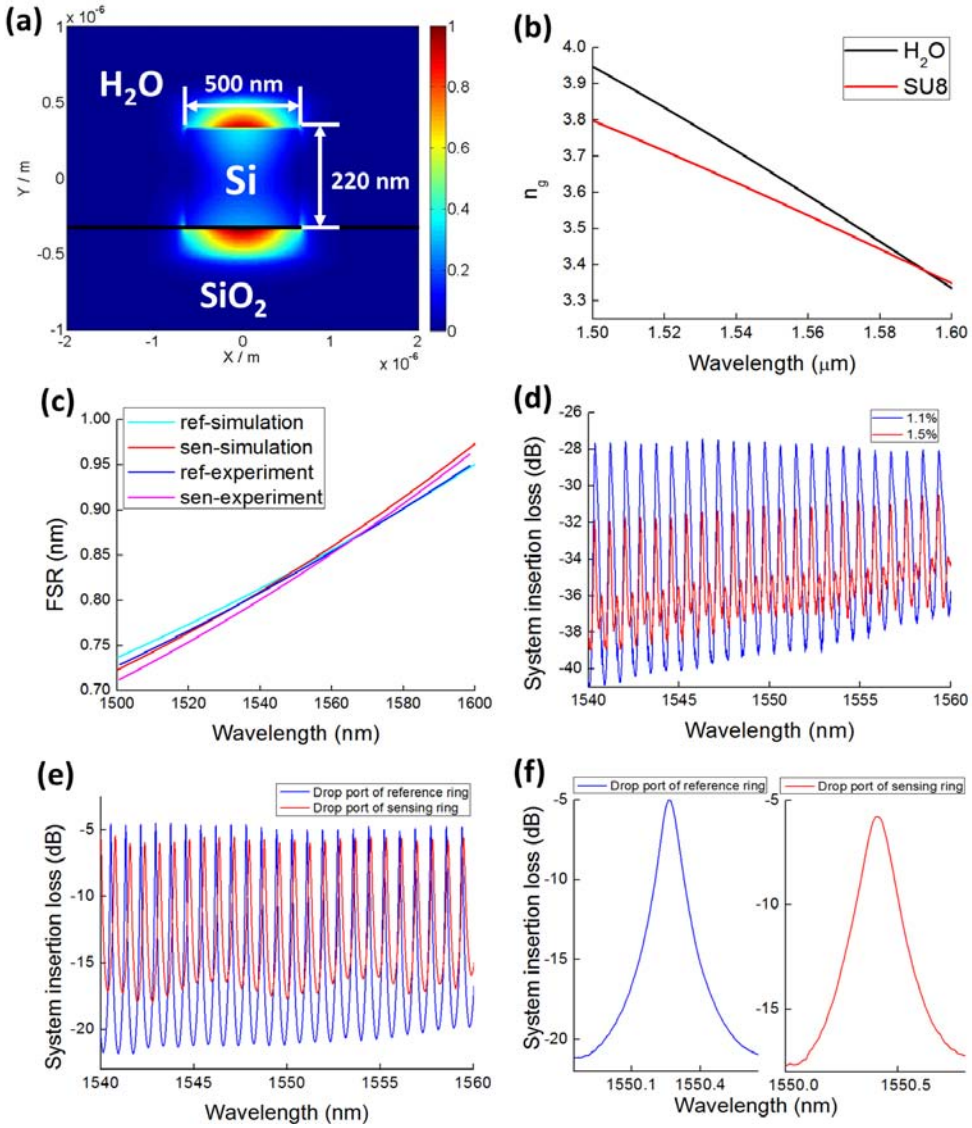

Fig. 4. (a) Electric field intensity of the waveguide for TM mode; (b) Group refractive index as a function of wavelength for the waveguide with H_2O and SU8 upper cladding respectively; (c) Simulated and experimental FSR of the CMRR; (d) Experimental transmission spectral of the drop port when the analyte is 1.1% and 1.5% NaCl aqueous solution respectively; (e) Experimental transmission spectral of the drop port for the reference ring and sensing ring; (f) Zoom in view of Fig. 4(e), the Q factor of sensing ring and reference ring is about 10336.06 at 1540.41 nm and 17225.11 at 1550.26 nm.

The distribution of the electric field intensity of the waveguide with the upper cladding of water for TM mode was simulated by the Finite Difference Eigenmode (FDE) as shown in Fig. 4(a). The height and width of the rib waveguide was set as 220 nm and 500 nm, respectively. The evanescent field on the surface is strongly influenced by the upper cladding, and contributes to high sensitivity of the sensor. The group refractive index (n_g) of the waveguide with different upper cladding was calculated as a function of wavelength, as

Optics EXPRESS

shown in Fig. 4(b). At 1550 nm, the refractive indices of H_2O and SU8 are 1.311 and 1.5753, respectively. The FSRr and FSRs are calculated according to the following formula,

$$\mathrm{FSR} = \frac{\lambda^2}{2\pi r \times n_g}, \tag{1}$$

where r is radius of the ring, λ is the wavelength. Figure 4(c) shows the simulated and experimental FSRr and FSRs of the CMRR. The values of FSRr and FSRs are similar to each other from 1550 to 1560 nm. The transmission spectra of the drop port for 1.1% and 1.5% NaCl aqueous solutions are shown in Fig. 4(d). The change of the analyte concentration influences the contrast of the transmission curve. The CMRR sensor is based on Vernier effect. Compared to a single microring resonator, the peak wavelength shift of the envelope function in the CMRR transmission is magnified by a factor of $\mathrm{M}=\frac{FSR_r}{|FSR_r - FSR_s|}$. When the FSRr and FSRs are equal, the envelop peak of the CMRR is difficult to be extracted for the wavelength interrogation. But the sensitivity for the intensity interrogation will be the highest [23]. Figure 4(e) shows that the Q of the individual ring is almost constant within the 3dB bandwidth of the broadband light source (~20 nm). From Fig. 4(f), the Q of the sensing ring and the reference ring is about 10336.06 at 1540.41 nm and 17225.11 at 1550.26 nm, respectively. For the individual ring resonator with higher Q factor, the extinction ratio is larger, implying that the dynamic range of the normalized output power is larger and the sensitivity of that CMRR is higher.

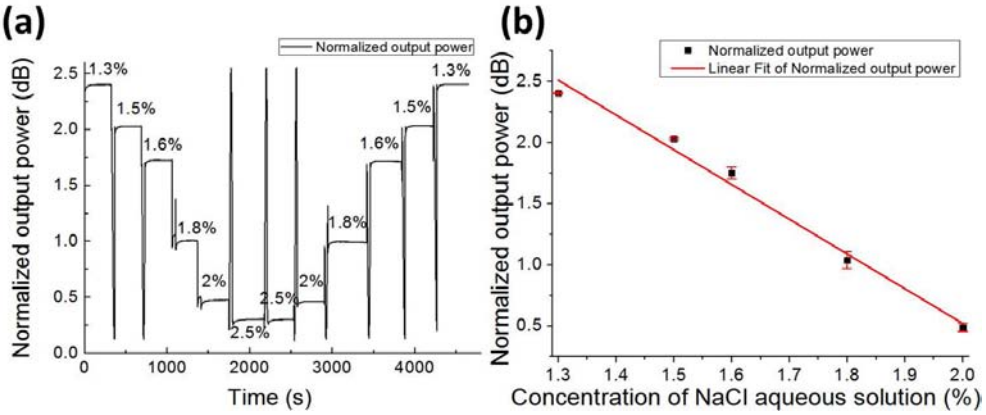

Fig. 5. (a) Time-dependent response of the output power with different concentrations of NaCl aqueous solution; (b) The function curve of the output power with the concentration of the NaCl aqueous solutions.

For the intensity interrogation, a broadband light source with the center wavelength of 1550 nm and 3 dB bandwidth of 20 nm was used in the experiment. The output of the sensor response was detected by the PDs. The signal of the PD voltage was then collected and recorded by the home-made SAC and software. The collected signal as a function of time was shown in Fig. 5(a). The mutation of the signal during the sample replacement process was caused by the air column in the pipe. When the concentration of the NaCl aqueous solutions changes from 1.3% to 2%, the collected signal data can be fitted with a linear curve as shown in Fig. 5(b). The red error bars obtained from three groups of NaCl aqueous solution for each concentration. The sensitivity of the system was measured to be S_v = 1579 dB/RIU by extracting the slopes of the curves, corresponding to a refractive index change about 1.8 × 10^{-3} RIU/% [15]. Accordingly, the LOD for the measurement of refractive index of the sensor is calculated based on the standard deviation σ = 0.0051297 dB divided by the sensitivity S_v,

Optics EXPRESS

i.e. LOD = $3\sigma/S_v$ = 9.7 × 10^{-6} RIU. The standard deviation σ is obtained from the time-dependent response measurement in DI water.

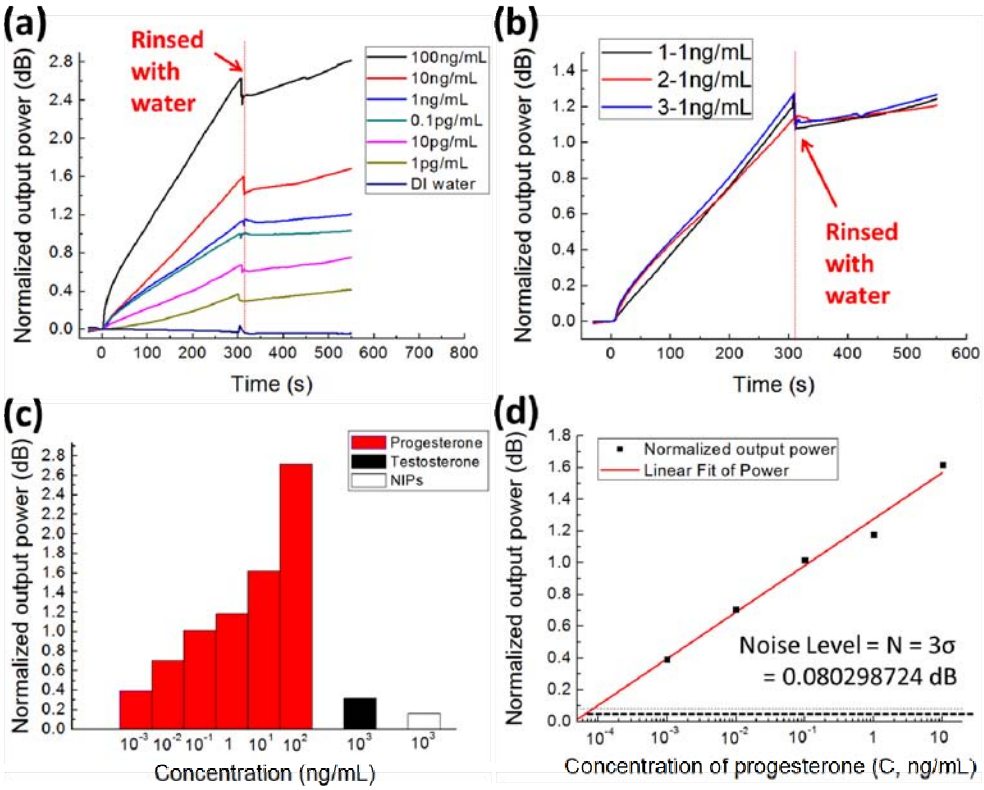

Fig. 6. (a) Time-dependent power change due to the affinity binding of progesterone at concentrations of 1 pg/mL, 10 pg/mL, 0.1 ng/mL,1 ng/mL, 10 ng/mL and 100 ng/mL in water; (b) Three groups of repeated experiments at concentrations of 1 ng/mL; (c) The response of different solution for the progesterone-MIPs CMRR chip (progesterone and testosterone) and NIPs (progesterone) at 500 seconds; (d) The linear fitting of power with the log values of the different concentrations of progesterone.

As a model experiment, we formed a MIPs-CMRR with the template molecule of progesterone and detected the response of the sample concentration, repeatability and specificity. For quantitative detection, different concentrations of progesterone aqueous solution were injected into the microfluidic channel for 5 min and then rinsed with DI water for 250 s. The sensor response for the sensor chips coated by the MIPs in the different concentrations of progesterone (from 0.001 ng/mL to 100 ng/mL) were shown in Fig. 6(a). The normalized output power rises gradually from 0 second to 300 second because of the progesterone binds specifically to the MIPs. And the mutational decline at time 300 second is due to the refractive index change from the analyte to water. Figure 6(b) shows the sensor response measured three times at concentration of 1 ng/mL. The standard deviation σ of the three group is σ = 0.026766241 dB, thus the noise level is N = 3σ = 0.080298724 dB. The red columns in Fig. 6(c) show the response for the detection of progesterone at concentration from 0.001 to 100 ng/mL at reaction time of 500 s (i.e. 200 s of rinsing with water). The power change increased with the concentrations of progesterone aqueous solutions. A control experiment on the measurement of testosterone shows a much lower response (2.741474 dB for 100 ng/mL of progesterone and 0.3152 dB for 1 μg/mL of testosterone) as compared with the specific progesterone binding, indicating the good specificity of the MIPs for the recognition of progesterone. In addition, NIPs for progesterone gives a negligible response as

Optics EXPRESS

compared with MIPs. Figure 6(d) shows the linear relationship of the sensor response ($P = 1.27563 + 0.2931 \times \lg C$, $R^2 = 0.98003$) with the log values of the different concentrations of progesterone. The slope of the fitting line is S = 0.2931 dB. The LOD was calculated to be 83.5 fg/mL, which is determined as the concentration of the sample with the response equal to the noise level. Compared with ELISA based sensor [24,25], the LOD of our sensor is three orders of magnitude lower. The CMMR sensor consists of the reference ring and the sensing ring. The sensitivity is determined by the lower Q of the two rings. The absorption of the sample deteriorated the Q of the sensing ring and the sensitivity of the CMRR. So the CMRR sensor can't measure the larger absorption or even opaque samples.

4. Conclusion

In summary, we report a refractive index sensing system based on SOI CMRR. The identical FSRs and FSRr were designed to achieve the largest sensitivity for intensity interrogation. A high sensitivity of 1579 dB/RIU, along with a refractive index LOD of 9.7×10^{-6} RIU was achieved. Compared with the traditional wavelength interrogation, our method doesn't require the narrow line width tunable lasers or the high-resolution optical spectrum analyzers. The reported sensor system provides an excellent candidate for low-cost and highly-sensitive optical biosensor systems. Furthermore, we modified the CMRR sensor with MIPs for the detection of progesterone which shows the LOD of 83.5 fg/mL.

Funding

National Natural Science Foundation of China (61535010, 21605116, 61605172); National High Technological Research and Development Program of China (2014AA06A504); Science and Technology Department of Zhejiang Province (2016C33074); Natural Science Foundation of Zhejiang Province (LY16F050001).

Acknowledgments

The authors acknowledge the wafer preparation and technical assistance by the Integrated Circuit Advanced Process Center (ICAC) of Institute of Microelectronics of Chinese Academy of Sciences (IMECAS).